Springer

Journal of Mechanical Science and Technology 22 (2008) 1651~1659

Journal of Mechanical Science and Technology

www.springerlink.com/content/1738-494x
DOI 10.1007/s12206-008-0704-2

Structural optimization for a jaw using iterative Kriging metamodels

Il-Kwon Bang[1], Dong-Seop Han[2], Geun-Jo Han[3] and Kwon-Hee Lee[4,*]

[1]*Graduate Student, Dept. of Mech. Eng., Dong-A University*
[2]*Contractor Professor of BK21 Project, Dept. of Mech. Eng., Dong-A University*
[3]*Professor, Dept. of Mech. Eng., Dong-A University*
[4]*Associate Professor, Dept. of Mech. Eng., Dong-A University, 604-714 Korea*

(Manuscript Received May 14, 2007; Revised April 5, 2008; Accepted July 10, 2008)

Abstract

Rail clamps are mechanical components installed to fix the container crane to its lower members against wind blast or slip. Rail clamps should be designed to survive harsh wind loading conditions. In this study, a jaw structure, which is a part of a wedge-typed rail clamp, is optimized with respect to its strength under a severe wind loading condition. According to the classification of structural optimization, the structural optimization of a jaw is included in the category of shape optimization. Conventional structural optimization methods have difficulties in defining complex shape design variables and preventing mesh distortions. To overcome the difficulties, a metamodel using the Kriging interpolation method is introduced to replace the true response by an approximate one. This research presents the shape optimization of a jaw using iterative Kriging interpolation models and a simulated annealing algorithm. The new Kriging models are iteratively constructed by refining the former Kriging models. This process is continued until the convergence criteria are satisfied. The optimum results obtained by the suggested method are compared with those obtained by the DOE (design of experiments) and VT (variation technology) methods built in ANSYS WORKBENCH.

Keywords: Container crane; Rail clamp; Jaw; Shape optimization; Kriging; DOE; VT

1. Introduction

The Korean peninsula has often come under the influence of strong typhoons. Since 2000, the powerful typhoons to hit Korea were Prapiroon in 2000, Rusa 2002, Maemi in 2003 and Nabi in 2005. Particularly, Maemi, meaning cicada in Korean and bringing record-breaking 60 m/s winds, was the second most powerful typhoon to hit Korea since 1904 when Korea began collecting weather data [1]. When Maemi howled into the major port of Busan, 11 heavy duty shipping cranes, weighing up to 985 tons, were toppled and twisted beyond recognition. It was reported that the damage was so severe that it could take up to one year and KRW 40 billion (almost USD 42 million) to repair the cranes [1, 2].

In response to this climate influence, the Ministry of Maritime Affairs & Fisheries in Korea strengthened the related regulations for facilities and equipment of ports in 2004. According to the amended regulations, a container crane in operating mode should be able to resist wind load at 40 m/s and in stowing mode wind load at 70 m/s [3]. Compared to the former regulations, each limit speed rose 20 m/s. Thus, the structures for facilities and equipment in ports are to be designed in consideration of harsh wind loads.

The trend now is to build large-scale container ships such as ULCS (Ultra Large Container Ship) in response to rise in trade. For example, the ULCS can manage 12,000 TEU. With this trend, the container

*Corresponding author. Tel.: +82 51 200 7638, Fax.: +82 51 200 7656
E-mail address: leekh@dau.ac.kr

cranes have become larger than former container cranes. The large-scale container crane justifies the high design cost. Thus, it is important to design its components to meet the previously mentioned regulations.

When a container ship approaches the quay, the container crane is moved and stopped on the rails to load and unload the containers. This is called the operating mode. Then, the mechanical component called the rail clamp is used to fix the crane on the rails. If the rail clamp cannot play its role, the crane will run on a rail, inevitably leading to an accident. When a container crane is set to a stowing mode, the crane is fixed by stowage pin and tie-down load. Since this study focuses on the design of a jaw in the rail clamp, the loading condition is derived from the wind load at operating mode [4, 5].

The wedge-typed rail clamp has different mechanisms appropriate for three operating stages [3]. In this research, the load at wedge-working stage is only considered as the loading condition since the wedge-working stage is the largest of the three operating stages. Jaws, which are designed considering the strength, play an important role in wedging the structural components. The FE (finite element) method is used to predict the strength performance of a jaw. Furthermore, a structural optimization scheme is adopted to determine the optimum shape of a jaw. According to the classification of structural optimization, the structural optimization of a jaw is included in the category of shape optimization since the FE model of the jaw is composed of solid elements. However, classical structural optimization methods [6, 7] have difficulties in defining complex shape design variables and preventing mesh distortions in the shape optimization process [8].

To overcome these difficulties, this research presents the shape optimization of a jaw using iterative Kriging interpolation method and simulated annealing algorithm. The Kriging models are utilized to replace the true structural responses. In this research, the responses are the weight of a jaw and the maximum stress acted on a jaw. The new Kriging models are iteratively constructed by refining the former Kriging models. This process is continued until the convergence criteria are satisfied. The optimization problem expressed by Kriging models is solved by adopting a simulated annealing algorithm.

In this study, the commercial software, ANSYS/WORKBENCH [9], is utilized to calculate the strength performance and to compare the optimum design of a jaw obtained by the suggested method with the DOE and VT methods.

2. FE analysis of jaw

2.1 Operation of wedge-typed rail clamp

Rail clamps are mechanical components installed to fix the container crane to its bottom against wind blast or slip. As shown in Fig. 1, two rail clamps are installed in a container crane. The wedge-typed rail clamp such as that shown in Fig. 2 is composed of a jaw, wedge, locker, hanger, jaw pad, roller and wedge frame. Its operating mechanism is divided into three stages: opening stage, initial clamping stage, and wedge-working stage [3, 4].

The opening stage is represented in Fig. 3(a). When the locker is lifted up in the opening stage, the angle between two jaws becomes larger, and then the rail clamp separates from the rail. Thus, in this stage, the container crane is moved. Initial clamping stage in

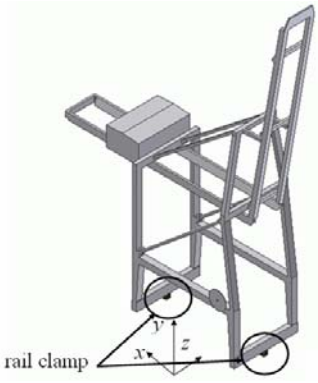

Fig. 1. A container crane.

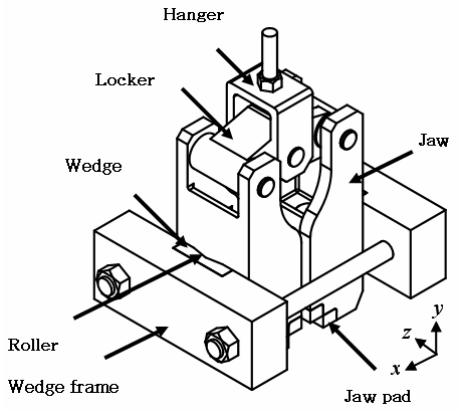

Fig. 2. Wedge-typed rail clamp.

Fig. 3(b) allows both jaw pads to put on the rail sides with small clamping force. That is, a container crane has a set position for working. This stage starts fixing the container crane and is operated by applying the force P. On the contrary, the wedge-working stage does not allow a container crane to move, because the clamping forces of both jaw pads increase as the wind speed increases.

The operating mechanism in the wedge-working stage is as follows [3, 4]: From the state of the initial clamping stage, the wedge frame attached to the container crane starts slipping when the z-directional wind load F_z is increased. Then, a V-shaped wedge built in the wedge frame makes the roller rotate along its slope, generating wedge action. As shown in Fig. 3(c), this wedge action results from the increase of the clamping force F_P applied on each jaw pad. The clamping forces prevent the container crane from slipping along the rail. In this research, the wedge-working stage is considered in the design of the jaw structure, because among the three stages, it generates the largest load.

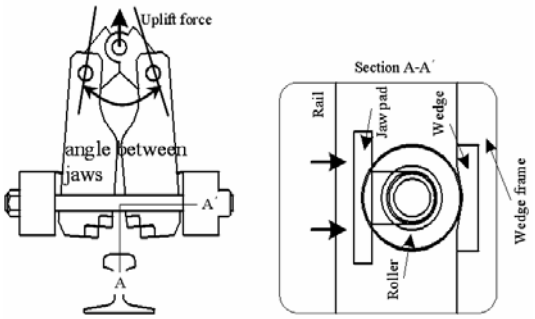

(a) Opening stage

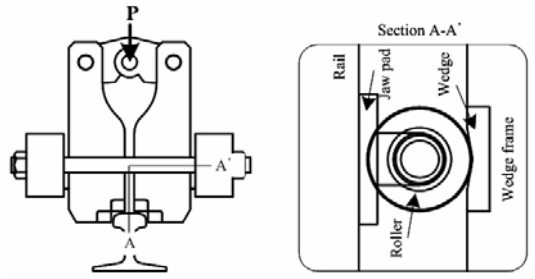

(b) Initial clamping stage

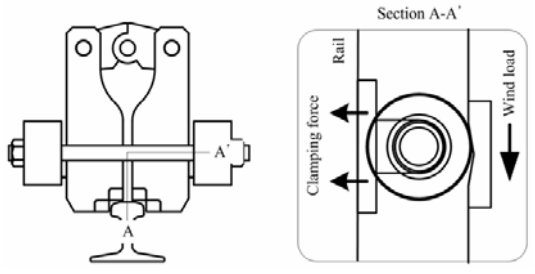

(c) Wedge-working stage

Fig. 3. Operating mechanism of wedge-typed rail clamp.

2.2 Finite element model and loading and boundary conditions

The regulations for the structural design of a container crane are specified in Specification for the Design of Crane Structures in KS, Load Criteria of Building Structure in Ministry of Construction & Transportation [3], Design Criteria of Cranes in BS2573 [10], etc. Since the British regulation evaluates the severest loading, this research adopted it in the load calculations.

According to the BS 2573, the z-directional wind load applied to the container crane of Fig. 1 is calculated as

$$F_z = C_{tz} \times q_h \times A_{unit} \times L \tag{1}$$

where C_{tz} and q_h are the wind load coefficients for wind load and wind pressure, and A_{unit} is the horizontal wind area per unit length, and L is the member length, respectively. By applying Eq. (1) to the container crane of Fig. 1, Eq. (1) is simplified as

$$F_z = 1.107 \times v_0^2 \tag{2}$$

where v_0 is the wind velocity. As mentioned in the Introduction, v_0 is set to 40 m/s.

Furthermore, there are two rail clamps in a container crane, and each one has two friction surfaces or two clamping surfaces. Thus, F_P is represented as

$$F_P = \frac{F_z}{4\mu_P} \tag{3}$$

where μ_P is the friction coefficient for the contact surface between jaw pad and rail. Thus, $F_z/4$ is equal to F_{zz} of Fig. 4.

From the above force analysis, we can derive the forces acting on a jaw. The free body diagram of a jaw can be represented as Fig. 4(a). In the wedge-working stage, F_P is generated on the jaw pads when the x-directional force of a roller F_{Rx} is applied to the

middle of the jaw and the locker supports the top of the jaw.

Considering the force equilibrium in Fig. 4(a), F_L and F_{Rx} are derived as

$$F_L = \frac{L_{JL}}{L_{JU}} \cdot F_P \tag{4}$$

$$F_{RX} = F_P + F_L = \left(1 + \frac{L_{JL}}{L_{JU}}\right) \cdot F_P . \tag{5}$$

Substituting the values of F_P, L_{JL} and L_{JU} to Eq. (5), F_{RX} is calculated as 1,110 kN. Furthermore, from the force equilibrium in Fig. 4(b), we can derive the value of F_{RZ}, that is, 197 kN. For the FE analysis of the jaw, we can assume that F_R is the external bearing load, the hole surface has fixed displacement in x direction, the surface A between the jaw pad and rail has fixed displacements in the x- and z- direction, and the surface B between the jaw pad and rail has a fixed displacement in the y-direction. The FE model meshed with tetrahedral elements is shown as Fig. 5 (a), while the stress contour at initial design is shown as Fig. 5(b).

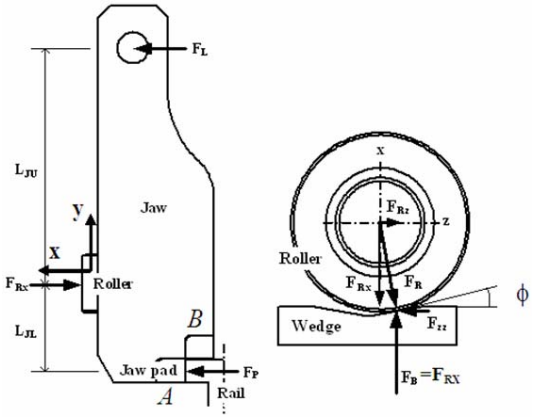

(a) Jaw (b) Roller & wedge

Fig. 4. Free body diagram of a jaw.

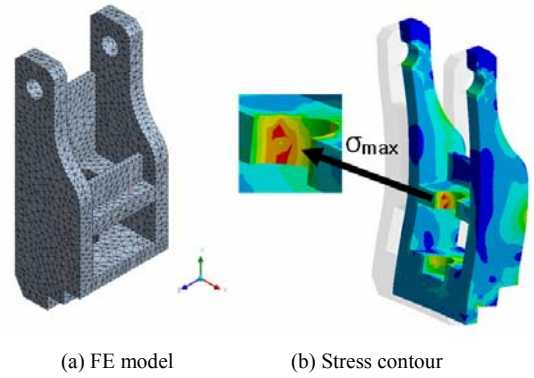

(a) FE model (b) Stress contour

Fig. 5. FE analysis of a jaw.

3. Optimization using the Kriging metamodel

3.1 Design variables and optimization formulation

The initial design satisfies the strength requirement; thus, the weight of a jaw can be reduced by structural optimization. As shown in Fig. 6, the design variables are set as the thicknesses of the structure (t_1, t_2 and t_3) and the length between the centers of the hole and curvature (l_1). In the initial design, t_1=30.0 mm, t_2=30.0 mm, t_3=85.0 mm and l_1=54.1 mm, and the weight of jaw is 43.5 kg. As shown in Fig. 5(b), the maximum stress of 533 MPa, which is calculated as the von Mises equivalent stress, is generated at the contact area between roller and jaw. The material for the jaw is SCM445, whose ultimate strength is 823 MPa. The maximum stress in the initial design was lower than the allowable stress for the safety factor of 1.5. Under the regulations of the Inspection Criteria for Facilities and Equipments in Port, the safety factor of the structure should be set to more than 1.5 [11].

Theoretically, the structural optimization for the jaw can be formulated as follows:

$$\textit{minimize} \quad w(t_1, t_2, t_3, l_1) \tag{6}$$

$$\textit{subject to} \quad \sigma_i - \sigma_a \le 0 , (i=1,\ldots,ne) \tag{7}$$

$$25 \text{ mm} \le t_1 \le 35 \text{ mm} \tag{8}$$

$$25 \text{ mm} \le t_2 \le 35 \text{ mm} \tag{9}$$

$$75 \text{ mm} \le t_3 \le 90 \text{ mm} \tag{10}$$

$$50 \text{ mm} \le l_1 \le 60 \text{ mm} \tag{11}$$

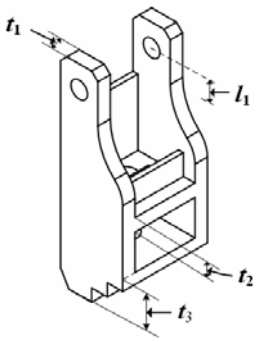

Fig. 6. Design variables of a jaw.

where w is the weight of the jaw, σ_i is the stress of the i-th element, σ_a is the allowable stress, and ne is the number of finite elements. The lower and upper bounds of each design variable are determined as its minimum and maximum values so as not to distort the meshed finite elements.

By observing Eqs. (6)-(11), it appears highly probable that the formulations can be easily solved. The best way to obtain its optimum shape is to adopt the classical structural optimization, in which a gradient-based optimization is utilized. This approach suggests that it is efficient to make the mapped meshes, but the mesh qualities in the initial design were bad around the round parts and the place where there is a maximum stress. Furthermore, its mesh qualities would become worsened when the design variables moved. To overcome the disadvantage of classical methods [6, 7], this research utilizes the metamodel called the Kriging model instead of the true model. In the DOE (design of experiments) stage, the FE mesh on each sample design point would be modified if the index such as aspect ratio, skewness, warpage or Jacobian value is not allowed. In this research, the FE model on each design point is re-meshed by using the ANSYS / WORKBENCH [9].

For this approach, Eqs. (6)-(7) are replaced by

$$\textit{minimize} \quad \hat{w}(t_1, t_2, t_3, l_1) \tag{12}$$

$$\textit{subject to} \quad \hat{\sigma}_{\max} - \sigma_a \le 0 \tag{13}$$

where ^ means the estimator of a response, and $\sigma_{\max}$ is the maximum stress generated at the jaw. Thus, two responses are approximated, using Kriging interpolation method.

3.2 Kriging interpolation method

Kriging is an interpolation method named after a South African mining engineer, D. G. Krige. Since the late 1990s, there have been attempts to apply the Kriging interpolation to optimization problems. This method for an approximation model is well explained in references [12-17]. Generally, the Kriging interpolation method provides a more reliable metamodel than response surface method when the response function is highly nonlinear.

In the Kriging model, the estimator for a true response $y(\mathbf{x})$ is represented as

$$\hat{y}(\mathbf{x}) = \hat{\beta} + \mathbf{r}^T(\mathbf{x})\mathbf{R}^{-1}(\mathbf{y} - \hat{\beta}\,\mathbf{q}) . \tag{14}$$

where $\mathbf{x}$ is the design variable vector, $\hat{\beta}$ is the estimated value of constant β, $\mathbf{R}^{-1}$ is the inverse of correlation matrix $\mathbf{R}$, $\mathbf{r}$ is the correlation vector, $\mathbf{y}$ is the observed data with n_s sample data, and $\mathbf{q}$ is the vector with n_s components of 1. In this research, $\mathbf{x} = [t_1, t_2, t_3, l_1]^T$ and y is the weight or maximum stress of a jaw. The correlation matrix and the correlation vector are defined as

$$R(\mathbf{x}^j, \mathbf{x}^k) = Exp\left[-\sum_{i=1}^{n} \theta_i \left| x_i^j - x_i^k \right|^2 \right],$$

(j=1,…, n_s, k=1,…, n_s). (15)

$$\mathbf{r}(\mathbf{x}) = [R(\mathbf{x},\mathbf{x}^{(1)}), R(\mathbf{x},\mathbf{x}^{(2)}), \ldots, R(\mathbf{x},\mathbf{x}^{(ns)})]^T \tag{16}$$

where n is the number of design variables. Thus, n is 4 in this study.

By differentiating the log-likelihood function with respect to β and σ^2, respectively, and setting them equal to 0, the maximum likelihood estimators of β and σ^2 are determined as Eqs. (17) and (18).

$$\hat{\beta} = (\mathbf{q}^T\mathbf{R}^{-1}\mathbf{q})^{-1}\mathbf{q}^T\mathbf{R}^{-1}\mathbf{y} , \tag{17}$$

$$\hat{\sigma}^2 = \frac{(\mathbf{y} - \hat{\beta}\,\mathbf{q})^T\mathbf{R}^{-1}(\mathbf{y} - \hat{\beta}\,\mathbf{q})}{n_s} . \tag{18}$$

In Eqs. (14)-(18), $\mathbf{R}$, $\mathbf{r}$, $\hat{\beta}$ and $\hat{\sigma}^2$ are functions of parameters θ_i (i=1,2,…,n). Thus when the parameters are determined, the approximated model can be constructed. Similarly to previous estimators, the unknown parameters of θ_1, θ_2,…, θ_n are calculated from the formulation as follows:

$$\textit{maximize} \quad -\frac{[n_s ln(\hat{\sigma}^2) + ln|\mathbf{R}|]}{2}, \tag{19}$$

where θ_i (i=1,2,…,n) > 0. In this study, the method of modified feasible direction is utilized to determine the optimum parameters. Finally, Eq. (14) is determined as the explicit form of design variables.

3.3 Design procedures

Step 1: DOE strategy

First, the sample points should be set up to obtain

the Kriging metamodel of weight and maximum stress. DOE strategies can be used to sample the design space. Depending on analysis time, the full combination, orthogonal array or Latin hypercube design can be selected as the sampling method. In this study, the orthogonal array is introduced to sample the design space.

Step 2: Matrix experiment

The responses of weight and maximum stress are calculated for each row of the orthogonal array. The number of experiments is identical to the number of rows in the orthogonal array. That is, an experiment means one finite element analysis. To avoid the mesh distortion, the FE model on each experiment is re-meshed.

Step 3: Building and validation of Kriging models

With the responses on the sample points, the Kriging model of each response is constructed. Therefore, two Kriging models are built since the number of responses is two. To assess the Kriging model, the error in the surrogate model is characterized by using a few metrics. In this research, the metric defined as Eq. (20) is utilized [14, 17].

$$CV = \sqrt{\frac{1}{n_s}\sum_{i=1}^{n_s}(y_i - \hat{y}_{\_i})^2} \tag{20}$$

where $\hat{y}_{\_i}$ is the i-th estimator of the Kriging model constructed without the i-th observation.

The metric CV should construct Kriging models as many as n_s , but this is a time-consuming process. In the reference [14], this process is reduced by using the calculated $\hat{\beta}$ and $\boldsymbol{\theta}$, and by calculating **R**, **r** and **f** with respect to n_s-1 sample points. However, this reduction is valid under the assumption that the elimination of one sample data has a negligible effect on the maximum likelihood estimates [14].

Step 4: Optimization using simulated annealing algorithm

Once an approximated formulation for optimization is obtained based on Kriging metamodels, a global optimization method such as tabu search method, simulated annealing algorithm or genetic algorithm can be employed to solve the design formulation. In this research, the simulated algorithm is adopted. In the calculation of the optimum, the computational cost is very low since all the true functions composing the optimization formulation are replaced by simple mathematical expressions.

To apply the simulated annealing algorithm, the objective and constraint functions as defined in Eqs. (12)-(13) are combined into a pseudo-objective function. Thus, the formulation for optimization can be reduced to

$$minimize \quad \psi(t_1, t_2, t_3, l_1) = \hat{w} + \alpha \cdot Max\left[0, (\hat{\sigma}_{\max} - \sigma_a)\right] \tag{21}$$

where α is a positive and large number reflecting the constraint feasibility of Eq. (13).

Step 5: Convergence criteria

The iterative process is stopped when the two convergence criteria are satisfied. The two convergence parameters are defined as

$$CP_1 = \frac{\left|\sigma^*_{\max} - \hat{\sigma}^*_{\max}\right|}{\sigma^*_{\max}} \times 100 \tag{22}$$

$$CP_2 = CV_{stress} \tag{23}$$

where $\hat{\sigma}^*_{\max}$ and $\sigma^*_{\max}$ are the estimated maximum stress and the true stress at the optimum determined from Eq. (21), and CV_{stress} is the CV of maximum stress, respectively. In this research, CP_1 and CP_2 should be less than 3% and 30MPa, respectively, and the corresponding values were derived experientially [16, 18-20].

If all the convergence criteria are satisfied, the design process is stopped. Otherwise, return to Step 1. Then, for a design variable, the design range between

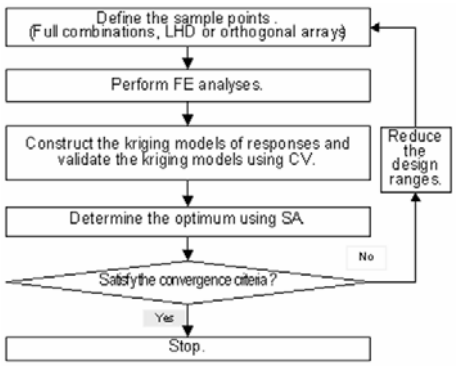

Fig. 7. Suggested design procedures.

lower and upper bounds is reduced. In this research, this range for the second iteration is fixed as 3mm, in reference to the optimum determined from Step 4. The value is determined experientially, considering the ratio of CP to its allowable value. If any finite element is distorted in the design range of a design variable, the finite element model should be re-meshed. The overall design process is represented in Fig. 7.

4. Results

4.1 Suggested method

The orthogonal array OA (2,7,49,8) [21] for Step 1 is adopted. OA means the orthogonal array, and the numbers in parentheses represent the strength, number of levels, number of rows, and number of columns, from left to right, respectively. Since there are four design variables in the jaw design, the last four columns in the arrays are empty. The levels of each design variable are generated by discretizing the design space equally. At the first iteration, the lower bound is set up as the first level, and the upper bound as the last level. The OA (2, 7, 49, 8), in which the level values are assigned, is represented in Table 1. For Step 2, the calculated responses are summarized in the last two columns of Table 1. The number of FE analyses is 49 since OA (2, 7, 49, 8) is utilized in Step 1.

Based on the responses of weight and maximum stress, a primitive Kriging model of each response is constructed by Step 3. The validations of the first Kriging models are summarized in Table 2. By applying Step 4, the optimum of Eqs. (12)-(13) is calculated. The predicted and true responses of weight and maximum stress at the optimum are summarized in Table 3, and the convergence criteria at the optimum are listed in Table 4. Since the first Kriging models cannot satisfy the criteria of Eqs. (22)-(23), the design procedure is iterated. That is, the levels of design variables are reduced to

$$23.5 \text{ mm} \le t_1 \le 26.5 \text{ mm} \quad (24)$$
$$27.5 \text{ mm} \le t_2 \le 30.5 \text{ mm} \quad (25)$$
$$81.0 \text{ mm} \le t_3 \le 84.0 \text{ mm} \quad (26)$$
$$54.0 \text{ mm} \le l_1 \le 57.0 \text{ mm} \quad (27)$$

The orthogonal array OA (2,7,49,8) for Step 1 and the responses in the second iteration are shown as Table 5. From Table 4, it is seen that the optimum determined from the second iteration satisfies the convergence criteria. Thus, the number of iterations to determine the optimum design in Fig. 7 is two.

In the first iteration of Table 3, the predicted maximum stress of the optimum design is the same as its allowable value, since the constraint related to the maximum stress is found as the active constraint. However, the true maximum stress of the optimum design has 2.1% error, which violates the allowable value. On the contrary, the predicted maximum stress of the second optimum design is not identical to the allowable value. However, there is very little difference between predicted and true maximum stresses. This difference may result from the local errors of the Kriging models. Compared to the true maximum stress at the second iteration, the predicted one has 0.6% error, and the true maximum stress is slightly less than the imposed allowable value. Compared with the initial design, the second optimum design reduces the weight by 17.3%.

Table 1. OA (2,7,49,8) experiments for the 1st iteration.

Exp. No.	t_1 (mm)	t_2 (mm)	t_3 (mm)	l_1 (mm)	w (kg)	σ_{max} (MPa)
1	25.0	25.0	75.0	50.0	36.9	747.9
2	25.0	26.7	77.5	53.3	37.5	655.3
. . .	. . .	. . .	. . .	. . .	. . .	. . .
48	35.0	33.3	82.5	53.3	48.1	484.0
49	35.0	35.0	80.0	56.7	47.9	509.9

Table 2. Validations of Kriging models for each iteration.

Iteration	Response	Optimum parameters				CV
		θ_1	θ_2	θ_3	θ_4	
1	w	0.596	1.295	1.278	0.545	
	σ_{max}	0.594	1.478	1.465	0.602	46.5
2	w	0.598	1.300	1.281	0.548	
	σ_{max}	9.762	1.448	1.437	9.770	23.8

Table 3. Optimum results for each iteration.

Iteration	Optimum design variables (mm)				Response (σ: MPa, w : kg)			
	t_1	t_2	t_3	l_1	$\hat{w}$	w	$\hat{\sigma}_{max}$	σ_{max}
1	25.0	29.0	82.5	55.0	38.3	39.6	548.0	560.0
2	23.5	28.4	82.5	55.5	38.2	37.1	542.0	545.2

Table 4. Convergence parameters for each iteration.

Iteration	Convergence parameter	
	CP_1	CP_2
1	6.9	46.5
2	2.5	23.8

Table 5. OA (2,7,49,8) experiments for the 2nd iteration.

Exp. No.	t_1 (mm)	t_2 (mm)	t_3 (mm)	l_1 (mm)	w (kg)	σ_{max} (MPa)
1	23.5	27.5	81.0	54.0	36.8	602.7
2	23.5	28.0	81.5	55.0	36.9	541.4
·	·	·	·	·	·	·
·	·	·	·	·	·	·
·	·	·	·	·	·	·
48	26.5	30.0	82.5	55.0	39.98	556.9
49	26.5	30.5	82.0	56.0	40.0	576.0

Table 6. Comparisons of results.

Method	Optimum design variables (mm)				Response (σ: MPa, w : kg)			
	t_1	t_2	t_3	l_1	$\hat{w}$	w	$\hat{\sigma}_{max}$	σ_{max}
DOE	27.0	27.6	81.5	59.0	39.8	39.8	537.6	525.0
VT	28.5	28.5	80.8	51.4	41.5	41.5	535.5	526.9
Suggested method	23.5	28.4	82.5	55.5	38.2	37.1	542.0	545.2

4.2 ANSYS workbebch

Two methods for shape optimization are built in the software [9]: the DOE method, and the VT method. The DOE method in the software adopts the central composite approach as the sampling method and the response surface approach as the approximation method. The VT method utilizes the first-order Taylor series as the approximation method.

Both of them have shortcomings in treating the highly nonlinear functions, even though they have the merit of reduction of computer run time, since the DOE and VT methods approximate a true function to linear and quadratic functions, respectively. To supplement these shortcomings, the DOE and VT methods supply three candidate designs. Then, the designer selects the optimum from thee candidate designs. Thus, the optimum design is a very intuitive one. The detailed processes are summarized in the reference [22].

From Table 6, it is seen that the DOE and VT methods reduced the weight only slightly but the suggested method reduced the weight greatly.

5. Conclusions

The following conclusions can be made from this study.

The present study proposes a structural optimization procedure applicable to the jaw design for a container crane based on Kriging approximate models and a simulated annealing algorithm. This procedure includes shape optimization, which has been the most difficult to apply in the structural design of a jaw.

Generally, the maximum stress becomes highly nonlinear since its position can be changed with respect to the design point. Adopting the Kriging model to surrogate the maximum stress is efficient. Finally, the approximate maximum stress represented by a Kriging model enables one to solve for shape optimization formulation by the simulated annealing algorithm.

The shape optimum design of a jaw is achieved by the Kriging approach and global optimization algorithm, which can consider severe wind loading condition. The weight at the optimum is decreased by around 17.3%, which is more than the optimal solutions of previous study. The results of the optimization presented in this paper can be applied to the design of another component in a container crane.

Acknowledgment

This study was supported by research funds from Dong-A University.

References

[1] Terra Daily, Typhoon Maemi kills 33 in South Korea, *http://www.terradaily.com/2003/030913080410.ucxbyd9l.html* (2003).

[2] J. R. Kim, Wind resistance design learning from typhoon Maemi, *J. Wind Engineering Institute of Korea (in Korean)*, 7 (2) (2003) 150-156.

[3] D. S. Han, A Study on the Structural Design of the Wedge Type Rail Clamp for a Container Crane, Ph. D. Dissertation, Dong-A University, Busan, Korea (2006).

[4] D. S. Han, G. J. Han, K. H. Lee and J. M. Lee, Design of the various wedge type rail clamp for quay crane according to the design wind speed criteria

changes, Proc. of Asia Navigation Conference, (2005) 291-301.

[5] S. W. Lee, J. J. Shim, D. S. Han, J. S. Park, G. J. Han, K. S. Lee and T. H. Kim, The effect of wind load on the stability of a container crane, *J. Korean Society for Precision Engineering (in Korean)* 22 (2) (2005) 148-155.

[6] MSC Software Corporation, MSC NASRAN 2004 Design Sensitivity and Optimization User's Guide, (2004) 123-124.

[7] VR & D, GENESIS Ver.6.0 Users Manual, Colorado Springs, USA, (2000).

[8] J. W. Shim and G. J. Park, Development of a structural shape optimization scheme using selective element method, *Trans. KSME A (in Korean)* 27 (12) 2101-2109.

[9] Taesung Software & Engineering Inc., ANSYS WORKBENCH Training Manual, Seoul, Korea, (2005).

[10] British Standards BS2573, Rules for the design of cranes specification for classification, stress calculations and design criteria for structures, UK. (1983).

[11] Ministry of Maritime Affairs & Fisheries, Management Regulation for Facilities and Equipment in Port, Seoul, Korea, (2004).

[12] J. Sacks, W. J. Welch, T. J. Mitchell and H. P. Wynn, Design and analysis of computer experiments, *Statistical Science* 4 (4) (1989) 409-435.

[13] A. Guinta and L. Watson, A comparison of approximation modeling techniques: polynomial versus interpolating models, Proc. of the 7th AIAA/ USAF/NASA/ISSMO Symposium on Multidisciplinary Analysis and Optimization, St. Louis, USA. 2 392-440 (1998) (AIAA-98-4758).

[14] D. R. Jones, M. Schonlau and W. J. Welch, Efficient global optimization of expensive black-box functions, *J. Global Optim.* 13 (4) (1998) 455-492.

[15] T. J. Santner, B. J. Williams and W. I. Notz, The Design and Analysis of Computer Experiments, Springer, New York, (2003).

[16] K. H. Lee and D. H. Kang, A robust optimization using the statistics based on kriging metamodel, *JMST.*20 (8) (2006) 1169-1182.

[17] S. W. Kim, J. J. Jung and T. H. Lee, Candidate points and representative cross-validation approach for sequential sampling, *Trans. KSME A (in Korean)* 31 (1) (2007) 55-61.

[18] K. H. Lee, Optimization of a driver-side airbag using kriging based approximation model, *JMST.* 19 (1) (2005) 116-126.

[19] K. H. Lee and G. J. Park, A global robust optimization using kriging based approximation model, *JSME Int. J. (C)* 49 (3) (2006) 779-788.

[20] K. H. Lee and D. H. Kang, Structural optimization of an automotive door using the kriging interpolation method, *Proc. of the Institution of Mechanical Engineers, Part D*: *J. Automobile Eng.* 221 (12) (2007) 1525-1534.

[21] G. Sherwood, On the construction of orthogonal arrays and covering arrays using permutation groups, http://home.att.net/~gsherwood/cover.htm (2006).

[22] I. K. Bang, D. H. Kang, D. S. Han, G. J. Han and K. H. Lee, Shape optimization for a jaw using design of experiments, *J. Korean Navigation and Port Research (in Korean)* 30 (8) (2006) 685-690.